Partitioning evapotranspiration based on the concept of underlying water use efficiency

Sha Zhou[1], Bofu Yu[2], Yao Zhang[3], Yuefei Huang[1,4], and Guangqian Wang[1]

[1] State Key Laboratory of Hydroscience and Engineering, Department of Hydraulic Engineering, Tsinghua University, Beijing, China, [2] School of Engineering, Griffith University, Nathan, Queensland, Australia, [3] Department of Microbiology and Plant Biology, Center for Spatial Analysis, University of Oklahoma, Norman, Oklahoma, USA, [4] College of Ecological and Environmental Engineering, Qinghai University, Xining, Qinghai, China

Correspondence to: Y. Huang, yuefeihuang@tsinghua.edu.cn

Abstract

Evapotranspiration (ET) is dominated by transpiration (T) in the terrestrial water cycle. However, continuous measurement of transpiration is still difficult, and the effect of vegetation on ET partitioning is unclear. The concept of underlying water use efficiency (uWUE) was used to develop a new method for ET partitioning by assuming that the maximum, or the potential uWUE is related to T while the averaged or apparent uWUE is related to ET. T/ET was thus estimated as the ratio of the apparent over the potential uWUE using half-hourly flux data from 17 AmeriFlux sites. The estimated potential uWUE was shown to be essentially constant for 14 of the 17 sites, and was broadly consistent with the uWUE evaluated at the leaf scale. The annual T/ET was the highest for croplands, i.e., 0.69 for corn and 0.62 for soybean, followed by grasslands (0.60) and evergreen needle leaf forests (0.56), and was the lowest for deciduous broadleaf forests (0.52). The enhanced vegetation index (EVI) was shown to be significantly correlated with T/ET and could explain about 75% of the variation in T/ET among the 71 site-years. The coefficients of determination between EVI and T/ET were 0.84 and 0.82 for corn and soybean, respectively, and 0.77 for deciduous broadleaf forests and grasslands, but only 0.37 for evergreen needle leaf forests. This ET partitioning method is sound in principle and simple to apply in practice, and would enhance the value and role of global FLUXNET in estimating T/ET variations and monitoring ecosystem dynamics.

1 Introduction

Evapotranspiration (ET), consisting of evaporation from wet surfaces (E) and transpiration through plants (T), is critical for global water cycle and energy balance. Transpiration is coupled with carbon assimilation, and exchanges of water and carbon between the atmosphere and terrestrial ecosystems play an essential role in global hydrological and carbon cycles. To partition ET into E and T and investigate the factors controlling ET partitioning would improve modeling of atmosphere-land surface interactions and help understand the biophysical processes involved [*Lawrence et al*., 2007]. The global T/ET was estimated to be $61 \pm 15\%$ based on MODIS-ET products, and the

evapotranspiration is dominated by transpiration in most terrestrial ecosystems, varying from its highest value in tropical rainforests ($70 \pm 14\%$) to the lowest in steppes, shrublands, and deserts ($51 \pm 15\%$) based on a meta-analysis of ET partitioning studies [*Schlesinger and Jasechko*, 2014]. Since transpiration accounts for a major portion of land surface evapotranspiration and is directly related to vegetation types and dynamics, terrestrial vegetation would thus have a strong influence on T/ET [*Wang et al*., 2014]. An increase in T/ET was reported as the vegetation cover was increased [*Ashktorab et al*., 1994; *Young et al*., 2009; *Wang et al*., 2010]. For example, experimental results showed that the T/ET increased from 0.61 to 0.83 when woody cover was increased from 25% to 100% using a stable isotopic technique [*Wang et al*., 2010]. However, the T/ET is difficult to measure in the field and it remains a challenge to continuously estimate T/ET in terrestrial ecosystems [*Kool et al*., 2014; *Schlesinger and Jasechko*, 2014]. It is therefore important to undertake comprehensive analyses of variations in T/ET and investigate the controlling effect of vegetation over T/ET in different ecosystems.

The stable isotope technique is a commonly used method for ET partitioning in arid environments with sparse vegetation [*Wang et al*., 2010, 2013; *Good et al*., 2014]. However, the isotope partitioning technique is costly and laborious, and is not suitable for agricultural and forest ecosystems when soil evaporation is small (<10%) [*Griffis*, 2013]. Eddy covariance is a widely used technique to measure the biosphere-atmosphere exchanges of carbon dioxide and water vapor, and the flux networks have been established globally [*Baldocchi*, 2014]. The flux data have been used to partition ET using different approaches. As a simple and intuitive method, the measured water fluxes from the canopy and understory were assumed to represent T and E, respectively [*Baldocchi and Ryu*, 2011]. This approach, however, ignores the evaporation due to rainfall interception by the canopy and the transpiration through understory plants, and is not applicable to nonforest ecosystems. The combined use of eddy covariance and sap flow techniques to estimate ET (and E) and T simultaneously provides a comprehensive method for ET partitioning [*Cammalleri et al*., 2013]. Nevertheless, the sap flow estimates are sensitive to the tower footprint, which may result in large discrepancy between the estimated E+T and ET, because species composition is not constant within the tower footprint which varies with wind direction and distance from the tower [*Wilson et al*., 2001]. The flux data were also used for ET partitioning using a correlation analysis method based on a flux-variance similarity assumption [*Scanlon and Sahu*, 2008; *Scanlon and Kustas*, 2010, 2012]. In spite of the widespread flux towers, the correlation analysis method was only adopted at a few sites and had not been widely used because the method required high frequency (10 Hz) eddy covariance data which were only available to tower owners and not widely shared. A simple method using widely available half-hourly flux data would contribute to ET partitioning for different ecosystems.

Using half-hourly data from 42 AmeriFlux sites, *Zhou et al*. [2014b] showed that ET is related to gross primary productivity (GPP) and vapor pressure deficit (VPD), and proposed an underlying water use efficiency (uWUE = $GPP \cdot VPD^{0.5}/ET$) model, and argued that the relationship between $GPP \cdot VPD^{0.5}$ and ET is nearly linear when soil evaporation is small and transpiration takes up a large portion of ET during the growing season. The effect of soil evaporation on the relationship between $GPP \cdot VPD^{0.5}$ and ET resulted in variations in uWUE both at half-hourly and daily time scales [*Zhou et al*., 2014b2015]. Since the variation in uWUE was attributed to the changes in T/ET, the uWUE model could be used for ET partitioning when the variations in uWUE are related to the relative portion of ET as T. While there are models to simulate ecosystem processes including primary bioproduction, and hydrologic balance such as *Running and Coughlan* [1988] to allow ET partitioning, and detailed examination of the complex relationships between GPP and water balance at a range of scales and in different regions [*Beer et al*., 2007; *Jasechko et al*., 2013], these approaches are not directly related to ET partitioning based on the concept of water use efficiency considered in the paper.

The fundamental difference between the processes of evaporation and transpiration is that transpiration is essentially associated with vegetation and evaporation only relies on the soil and environmental conditions, thus, vegetation is considered as the first-order factor affecting ET partitioning [*Scanlon and Kustas*, 2012]. In previous studies, leaf area index (LAI) was used to analyze the relationship between vegetation cover and T/ET. Using a tow-source model, *Wang and Yamanaka* [2014] suggested that LAI was the primary controlling factor of the seasonal variations in T/ET and there was a logarithmic relationship between LAI and T/ET. *Wang et al*. [2014] also showed that LAI and growing stage could explain 43% of the variations in T/ET using an exponential function based on 334 published global data sets. In addition to LAI, other vegetation indices, such as normalized difference vegetation index (NDVI), soil adjusted vegetation index (SAVI), and enhanced vegetation index (EVI) derived from remote sensing data, were widely used to monitor continuous vegetation dynamics and ecosystem responses to environmental change [*Ferreira et al*., 2003; *Zhang et al*., 2003; *Zhou et al*., 2014a]. It was shown that EVI was linearly correlated with SAVI [*Gao et al*., 2000], and was superior to NDVI in vegetation monitoring, and was more closely correlated with ET than NDVI [*Nagler et al*., 2005a2005b], thus, EVI was widely used in estimating ET [*Wang et al*., 2007; *Nagler et al*., 2009; *Murray et al*., 2009]. In addition, SAVI and EVI were found to be linearly correlated with the crop coefficient ($ET_{crop}/ET_{reference}$) and plant transpiration coefficient (i.e., T/ET) [*Choudhury et al*., 1994; *Glenn et al*., 2010, 2011]. An exploratory data analysis (results not shown) indicated that the correlation coefficient between EVI and our estimated T/ET was consistently higher than that between MODIS LAI and T/ET for a majority (>80%) of site-years.

Therefore, EVI as a surrogate variable could be used to develop a relationship between vegetation cover and T/ET.

This study has two broad objectives. The first was to develop a simple method to estimate T/ET using the concept of uWUE and the widely accessible half-hourly flux tower measurements. To provide a rationale and support for the proposed method for ET partitioning, two auxiliary objectives of this study were to test whether the uWUE model of *Zhou et al*. [2014b] is broadly consistent at the leaf and ecosystem scales; and to test whether the maximum of uWUE for a growing season remains essentially constant over time for a given vegetation type. The second main objective of the study was to estimate the effect of vegetation on T/ET using the EVI as an indicator of vegetation cover for different ecosystems. Results in relation to the first main objective and the two auxiliary objectives are presented in sections 3.1 and 3.2. Results on the effect of vegetation on T/ET are presented in section 3.3. With widely available flux data, our proposed and validated method for ET partitioning would allow estimation and characterization of T/ET and its temporal variations at the local, regional, and global scales.

2 Data and Methods

2.1 Flux Tower Data

Flux tower data from 17 sites (71 site-years) from the Ameriflux network (http://public.ornl.gov/ameriflux) were used in this study (Table 1). There were four vegetation types with relatively high vegetation coverage during the growing season, including croplands (CRO), deciduous broadleaf forests (DBF), evergreen needle leaf forests (ENF), and grasslands (GRA). Four of the five sites for croplands were located on agricultural land with annual corn (C4)-soybean (C3) rotation. Half-hourly flux and meteorological data were used, including net solar radiation (Rn, $W \cdot m^{-2}$), air temperature (TA, °C), latent heat flux (LE, $W \cdot m^{-2}$), VPD (hPa), and estimates of GPP ($g\ C \cdot m^{-2} \cdot d^{-1}$). Using the TA and LE data, measurements of ET ($kg\ H_2O \cdot m^{-2} \cdot d^{-1}$) were calculated at half-hourly intervals [*Donatelli et al*., 2006]. The eddy covariance flux measurements were friction velocity (USTAR) filtered and gap-filled using the Artificial Neural Network method, and were divided into four categories, i.e., the original, most reliable, medium and least reliable data according to data quality [*Reichstein et al*., 2005].

Table 1. Information on the 17 Ameriflux Sites Used in This Study[a]

	Lat	Long	ID	PFT	Period of Record	$uWUE_p$	Reference
1	40.006	−88.29	US-Bo1	CRO (corn)	2001/2003/2005	22.32	*Hollinger et al.* [2005]
				CRO (soybean)	2000/2002/2004/2006	14.74	
2	41.859	−88.223	US-IB1	CRO (corn)	2006	19.96	*Matamala et al.* [2008]
				CRO (soybean)	2005/2007	13.63	
3	41.165	−96.477	US-Ne1	CRO (corn)	2001–2005	19.18	*Suyker et al.* [2005]
4	41.165	−96.47	US-Ne2	CRO (corn)	2001/2003/2005	18.66	*Suyker et al.* [2005]
				CRO (soybean)	2002/2004	11.62	
5	41.18	−96.44	US-Ne3	CRO (corn)	2001/2003/2005	20.46	*Suyker et al.* [2005]
				CRO (soybean)	2002/2004	11.90	
6	42.538	−72.172	US-Ha1	DBF	2000–2006	21.25	*Urbanski et al.* [2007]
7	38.744	−92.2	US-Moz	DBF	2005–2007	15.09	*Gu et al.* [2007]
8	45.56	−84.714	US-UMB	DBF	2000–2003/2005–2006	13.73	*Gough et al.* [2008]
9	45.806	−90.08	US-WCr	DBF	2000/2002–2003/2005	14.12	*Yi et al.* [2004]
10	55.912	−98.382	CA-NS3	ENF	2004–2005	12.21	*Goulden et al.* [2006]
11	55.863	−98.485	CA-NS5	ENF	2002–2005	11.57	*Goulden et al.* [2006]
12	35.803	−76.668	US-NC2	ENF	2005–2006	13.65	*Noormets et al.* [2010]
13	35.55	−98.04	US-ARb	GRA	2005–2006	14.28	*Huang et al.* [2010]
14	35.547	−98.04	US-ARc	GRA	2005–2006	11.57	*Huang et al.* [2010]
15	34.25	−89.97	US-Goo	GRA	2002–2004, 2006	12.99	*Wilson and Meyers* [2007]
16	38.413	−120.951	US-Var	GRA	2001–2007	13.93	*Xu and Baldocchi* [2004]
17	37.521	−96.855	US-Wlr	GRA	2002–2004	11.89	*Coulter et al.* [2006]

[a]For each site, Latitude (Lat, °), Longitude (Long, °), Site Identifier (ID), Plant Functional Type (PFT), Period of Record, the potential uWUE ($uWUE_p$, g C·hPa$^{0.5}$/kg H_2O), and reference are presented. PFTs were taken from the International Geosphere-Biosphere Program (IGBP) land cover classification scheme (CRO = croplands, DBF = deciduous broadleaf forests, ENF = evergreen needle leaf forests, GRA = grasslands).

Data screening and quality control were performed to select half-hourly observations following a similar process described in *Zhou et al*. [2014b2015]. First, defective entries were excluded and only daylight data (7 A.M. to 7 P.M.) with positive Rn, GPP, ET, and VPD were used. Second, data from rainy days and several days that followed rainy days were excluded using the method in *Zhou et al*. [2015]. Third, only the half-hourly flux data with high confidence, i.e., original or most reliable data according to the quality flags were used. Fourth, data during the growing season were selected for each site, i.e., the data from days when the average half-hourly GPP was at least 10% of the 95th percentile of all the half-hourly GPP for the site. Finally, half-hourly data were used for ET partitioning at three time scales, i.e., daily, 8 day and site-year scales. Daily and 8 day T/ET values were estimated only for days when there were at least 10 effective entries and for 8 days when there were at least 80 effective entries, respectively.

2.2 Remote Sensing Data

To analyze the controlling effect of vegetation coverage over evapotranspiration partitioning, enhanced vegetation index (EVI) was used to represent the green vegetation coverage at the 17 sites in this study. The Moderate Resolution Imaging Spectroradiometer (MODIS) onboard the Terra satellite has provided continuous observations of terrestrial vegetation since March 2000. The MODIS Land Surface Reflectance 8 day 500 m product (MOD09A1, Collection 5) was used to generate 8 day EVI at a 500 m

resolution. Time series of the MOD09A1 data for each flux tower site were retrieved from the MODIS data portal at the Earth Observation and Modeling Facility (EOMF), University of Oklahoma (http://eomf.ou.edu/visualization/gmap/). The EVI was then calculated using the following equation [*Huete et al*., 2002]:

$$EVI = 2.5 \frac{\rho_{nir} - \rho_{red}}{\rho_{nir} + (6 \times \rho_{red} - 7.5 \times \rho_{blue}) + 1} \quad (1)$$

where ρ_{nir}, ρ_{red}, ρ_{blue} are the surface reflectance at near-infrared, red, and blue bands, respectively. According to the quality flags of MOD09A1, bad-quality observations, i.e., data with cloud or aerosol contamination were eliminated and filled using a three-step gap-filling method [*Jin et al*., 2013]. Once processed, 8 day EVI values for the 71 site-years were collated for comparison with the 8 day T/ET values estimated from the flux tower data. Linear regression between EVI and T/ET was attempted for each site-year for the four vegetation types to evaluate the controlling effect of vegetation coverage on T/ET and evaluate the strength of EVI in predicting T/ET.

2.3 Evapotranspiration Partitioning

Evapotranspiration (ET) consists of two components, namely vegetation transpiration (T) and soil evaporation (E). The essential distinction between the two components is that the former is related to leaf stomatal conductance as well as CO_2 assimilation (A). Thus A (μmol·m^{-2}·s^{-1}) and T (μmol·m^{-2}·s^{-1}) can be described following a stomatal conductance model [*Beer et al*., 2009; *Zhou et al*., 2014b]:

$$A = g_s \frac{(c_a - c_i)}{p_a} \quad (2)$$

$$T = 1.6 \cdot g_s \frac{(e_i - e_a)}{p_a} \quad (3)$$

where g_s is the stomatal conductance of CO_2 (μmol·m^{-2}·s^{-1}), and p_a the atmospheric pressure (hPa). $(c_a - c_i)$ and $(e_i - e_a)$ are the pressure difference between ambient air and inner leaf for CO_2 and that between inner leaf and ambient air for water vapor (hPa), respectively. The factor 1.6 in equation 3 exists because of a higher diffusion rate of water vapor than CO_2.

Water use efficiency at the leaf scale, i.e., the ratio of A over T is shown in equation 4 when $(e_i - e_a)$ is approximated by atmospheric vapor pressure deficit (VPD).

$$\frac{A}{T} = \frac{c_a(1 - \frac{c_i}{c_a})}{1.6\ VPD} \quad (4)$$

T is linearly dependent on VPD, and A is also affected by VPD since $(1 - c_i/c_a)$ (or $(1 - C_i/C_a)$ in mole fraction) is proportional to the square root of VPD (or D in mole fraction), as shown in equation 5 [*Lloyd*, 1991; *Lloyd and Farquhar*, 1994]:

$$1-\frac{C_i}{C_a}=\sqrt{\frac{1.6D(C_a-\Gamma)}{\lambda_{cf}C_a^2}} \quad (5)$$

where Γ is the leaf CO_2 compensation point, λ_{cf} represents the marginal water cost of carbon gain. The underlying water use efficiency at the leaf scale ($uWUE_i$) was then proposed taking into account the effect of VPD on water use efficiency [*Zhou et al*., 2014b]:

$$uWUE_i=\frac{A\sqrt{VPD}}{T} \quad (6)$$

Combining the equations 4-6, $uWUE_i$ is determined by $(C_a-\Gamma)$ and λ_{cf} as follows:

$$uWUE_i=\sqrt{\frac{C_a-\Gamma}{1.6\lambda_{cf}}} \quad (7)$$

Since changes in $(C_a-\Gamma)$ are much smaller than those in other variables, and λ_{cf} is almost constant within a certain vegetation type based on a model of optimal stomatal behavior [*Cowan and Farquhar*, 1977; *Lloyd*, 1991; *Lloyd and Farquhar*, 1994], thus $A\sqrt{VPD}$ is linearly correlated with T and $uWUE_i$ is approximately constant at the leaf scale.

From the leaf scale to the ecosystem scale, VPD is almost the same within a uniform environment, and the accumulation of carbon assimilation is represented by gross primary productivity (GPP), which is derived from the net ecosystem exchange and ecosystem respiration using the eddy covariance technique. However, it is not easy to observe T directly at the ecosystem scale and ET could be estimated from latent heat flux measurements, thus, ET was used to calculate uWUE at the ecosystem scale [*Zhou et al*., 2014b2015]. Here, we define a potential uWUE, $uWUE_p$ and an apparent uWUE, $uWUE_a$ at the ecosystem scale as follows:

$$uWUE_p=\frac{GPP\sqrt{VPD}}{T} \quad (8)$$

$$uWUE_a=\frac{GPP\sqrt{VPD}}{ET} \quad (9)$$

$uWUE_p$ is identical to $uWUE_i$ when applying the coupled carbon-water relationship in equation 6 to all the leaves, and they are nearly constant under steady state conditions within a uniform ecosystem, as shown in equation 7. Testing the broad consistency in the underlying water use efficiency at leaf and ecosystem scales was the first auxiliary objective of the study. $uWUE_a$ is the observed uWUE which is affected by soil evaporation and has been called simply as the underlying water use efficiency (uWUE) in previous research [*Zhou et al*., 2014b2015]. Thus, the ratio of transpiration over evapotranspiration, i.e., T/ET can be determined by the ratio of $uWUE_a$ over $uWUE_p$ as follows:

$$\frac{T}{ET}=\frac{uWUE_a}{uWUE_p} \quad (10)$$

or

$$T = \left(\frac{uWUE_a}{uWUE_p}\right) ET \quad (11)$$

When soil evaporation is negligible and T is close to ET, i.e., $T/ET \approx 1$, $uWUE_a$ is approximately equal to $uWUE_p$. Though ET could be derived from latent heat observations using the eddy covariance technique, we cannot measure T or T/ET directly, thus, $uWUE_a$ and $uWUE_p$ can provide a novel method to estimate T/ET hence T at the ecosystem scale. T/ET was widely shown to follow a single-peak diurnal pattern and the diurnal peak value would reach unity when vegetation coverage is high and soil evaporation is negligible [*Villegas et al*., 2014; *Wang and Yamanaka*, 2014; *Zhu et al*., 2015]. Here we assume that $uWUE_p$ is constant for each flux site, and $uWUE_a$ reaches its maximum value, namely $uWUE_p$, when T is equal to ET for terrestrial ecosystems with high vegetation coverage during the growing season. Thus, both $uWUE_a$ and $uWUE_p$, and hence T/ET can be estimated from half-hourly GPP, ET and VPD measurements. Testing the constancy of the $uWUE_p$, for a given vegetation type was the second auxiliary objective of the research.

2.4 Estimation of the Potential and Apparent uWUE

The $uWUE_p$ and $uWUE_a$ were estimated with half-hourly GPP, ET, and VPD data using the quantile regression and the linear regression methods, respectively. The linear regression technique was used extensively to develop the uWUE model and to evaluate alternative model formulations [*Zhou et al*., 2014b2015]. The least square, unbiased estimate of the slope of the regression line was in fact a flux-weighted estimate of $uWUE$, hence T/ET, with the weight being the flux squared (ET^2). The quantile regression method is appropriate for estimating multiple change rates from minimum to maximum responses, and can provide the regression slopes between the response and predictor variables on a series of quantiles [*Cade and Noon*, 2003]. The extreme quantiles, i.e., 5th and 95th quantiles were widely used to capture the lower and upper limits for the regression slopes [*Yu and Moyeed*, 2001; *Bremnes*, 2004; *Wang et al*., 2014]. In this study, quantile regression for the 95th percentile was used to estimate the upper bound of the ratio of $GPP \cdot VPD^{0.5}$ over ET, i.e., the $uWUE_p$ for each site. Both of the quantile regression and the linear regression passed through the origin to be consistent with the condition of zero GPP when stomata were totally closed. The long-term average $uWUE_p$ for each site was estimated using all the half-hourly flux data. For the four corn-soybean rotation site, the long-term average $uWUE_p$ was estimated separately for corn and soybean. For each site, an annual $uWUE_p$ for each site-year was also estimated for comparison with the long-term average $uWUE_p$ in order to test the assumption that $uWUE_p$ is essentially constant for a given vegetation type at each flux site. The $uWUE_a$ was estimated using the linear regression technique at three time scales, i.e., daily, 8 day, and site-year scales using half-hourly data at the corresponding time periods. For example, a time series of 8 day $uWUE_a$ would

be obtained by applying the linear regression to the half-hourly data from each non-overlapping 8 day period.

With the site US-ARc as an example, the long-term average $uWUE_p$ was estimated as the regression slope for the 95th quantile regression using all the half-hourly data for the site and the regression slope using half-hourly data for a particular 8 day period was estimated to represent a typical 8 day $uWUE_a$ value for the site. As shown in Figure 1a, the slope of the 95th quantile regression line, i.e., the long-term average $uWUE_p$ was 11.57 g C·hPa$^{0.5}$/kg H_2O for this site (US-ARc). The linear regression slope was 6.57 g C·hPa$^{0.5}$/kg H_2O for day of year 161–168 in 2005. Thus, the T/ET ratio was estimated to be 0.57 (=6.57/11.57) for the 8 day period (Figure 1b). It is clearly seen from Figure 1a that there is a linear upper bound between GPP·VPD$^{0.5}$ and ET, and the 95th quantile slope can effectively represent the largest marginal change in GPP·VPD$^{0.5}$ when ET is changed. Thus, the quantile regression could be used to estimate $uWUE_p$ using half-hourly data for flux sites. As is shown in equations 6 and 8, $uWUE_p$ at the ecosystem scale was assumed to be identical to $uWUE_i$ at the leaf scale. Since $uWUE_i$ can be calculated with λ_{cf} and $(C_a-\Gamma)$, equation 7 can be used to test whether the $uWUE_p$ estimated using the quantile regression technique was broadly consistent with $uWUE_i$. λ_{cf} derived from leaf gas exchange studies for different biomes of C3 plants in *Lloyd and Farquhar* [1994] was used to calculate $uWUE_i$ in this study. As there was no λ_{cf} data for corn, $uWUE_p$ was compared with $uWUE_i$ for C3 plants only, namely croplands, forests, and grasslands. The atmospheric CO_2 concentrations in the 2000s were about 380 ppm according to NOAA Mauna Loa CO_2 measurements, and the CO_2 compensation point was about 50 ppm for C3 plants [*Tans*, 2015; *Vogan and Sage*, 2012].

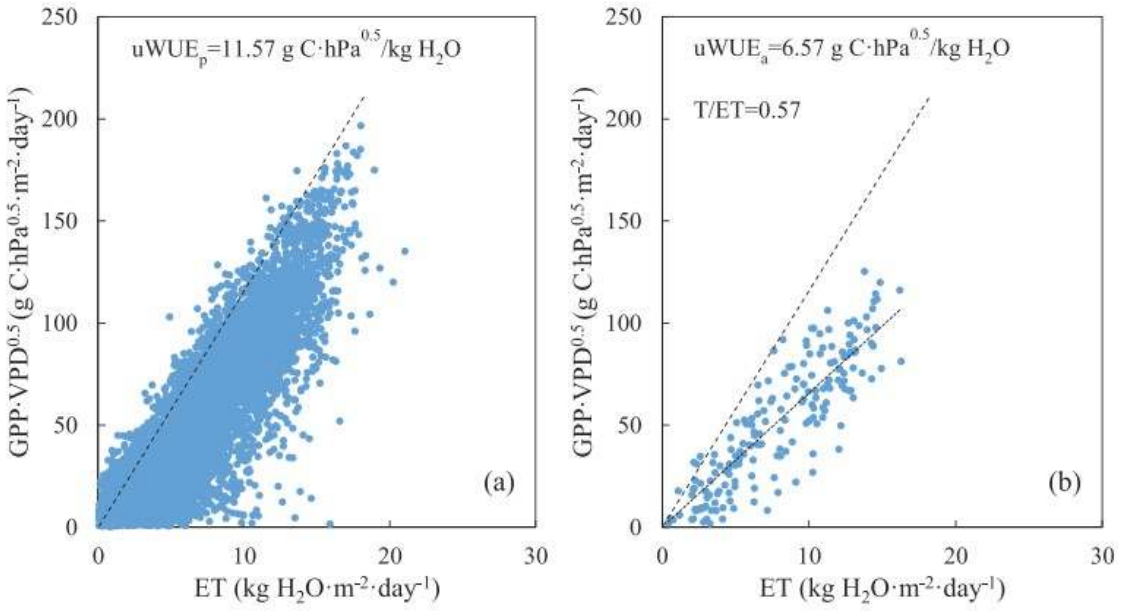

Figure 1. The 95th quantile regression using all the half-hourly data for the US-ARc site (a) and the linear regression using half-hourly data from day of year 161–168 in 2005 (b). The intercept was set to zero for both quantile and linear regressions.

3 Results and Discussion

3.1 Estimation and Validation of the Potential uWUE

The long-term average $uWUE_p$ for the 17 sites is shown in Table 1. At the five sites for croplands, corn (C4) years present much higher long-term average $uWUE_p$ than soybean (C3) years because C4 plants have intrinsically higher photosynthetic capacity and water use efficiency than C3 plants [*Ehleringer and Bjorkman*, 1977; *Furbank and Taylor*, 1995]. The long-term average $uWUE_p$ was 20.11 g C·hPa$^{0.5}$/kg H$_2$O for the five corn sites and 12.97 g C·hPa$^{0.5}$/kg H$_2$O for the four soybean sites. For natural vegetation, deciduous broadleaf forests (16.05 g C·hPa$^{0.5}$/kg H$_2$O) have a higher long-term average $uWUE_p$ than grasslands (12.93 g C·hPa$^{0.5}$/kg H$_2$O) and evergreen needle leaf forests (12.48 g C·hPa$^{0.5}$/kg H$_2$O). Figure 2 shows a comparison of the long-term average and annual $uWUE_p$ within a site. The annual $uWUE_p$ values were expressed in term of their departures from the long-term mean in percent (Figure 2a). The departure from the mean was less than 10% for a majority of the site-years (48 out of 71). The standard deviation of annual $uWUE_p$ was less than 1.0 g C·hPa$^{0.5}$/kg H$_2$O for 9 of the 17 sites, and the coefficient of variation was less than 0.1 for 13 sites (Figure 2b). However, the standard deviation of annual $uWUE_p$ was more than 2.0 g C·hPa$^{0.5}$/kg H$_2$O for three sites, i.e., US-Ha1 (DBF), US-Bo1 (CRO), and US-WCr (DBF), and the departure from the mean was more than 20% for several site-years at these three sites. A commercial harvest took place 300 m to the south-southeast of the tower in the summer of 2000 at the US-Ha1 site, and 42.8 m^3·ha^{-1} of the timber and 22.5 Mg C·ha^{-1} of aboveground woody biomass were removed from an area of 43 ha [*Urbanski et al*., 2007]. Thus, the biomass at the site was greatly

decreased in 2000 and this was gradually recovered since, resulting in a large variation in the estimated annual $uWUE_p$ from 2000 to 2006. The standard deviation of annual $uWUE_p$ for the site has markedly reduced in later years, from 4.46 g C·hPa$^{0.5}$/kg H_2O for the period 2000–2006 to only 1.1 g C·hPa$^{0.5}$/kg H_2O over the period 2003–2006. For the US-Bo1 site, corn and soybean rotation was within 50 m of the tower location, however, corn and soybean each occupied half of the area within 500 m of the tower location [*Meyers and Hollinger*, 2004]. Since the $uWUE_p$ was much larger for corn than soybean (Table 1), the mixed composition of corn and soybean may lead to great variations in annual $uWUE_p$ at the US-Bo1 site. The large standard deviation for the US-WCr site was attributed to the abnormally high $uWUE_p$ value of 20.81 g C·hPa$^{0.5}$/kg H_2O in 2003, which was much higher than what is expected for C3 plants, i.e., 11.77 ± 0.99 g C·hPa$^{0.5}$/kg H_2O for other 3 years. *Desai et al*. [2005] reported that ET declined greatly from 2002 to 2003 when precipitation decreased from 995 to 625 mm, however, the GPP increased for the same period from 2002 to 2003. The reason for the increased GPP during dry conditions in 2003 is not clear [*Desai et al*., 2005]. Since $uWUE_p$ was relatively stable for the remaining sites, it is reasonable to assume that the long-term average $uWUE_p$ is essentially constant for each site in order to estimate T/ET using the concept of the underlying water use efficiency.

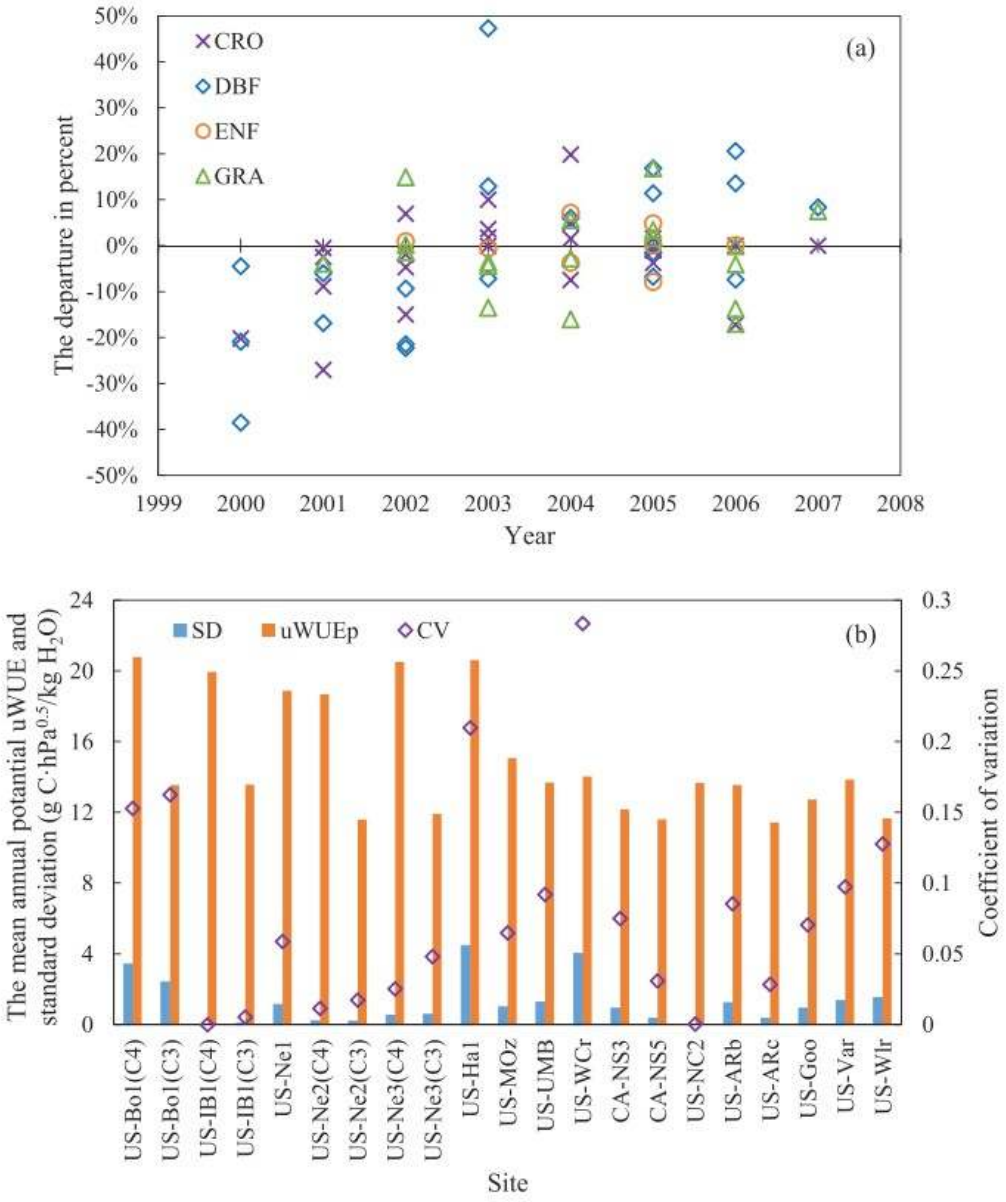

Figure 2. (a) The departures of annual $uWUE_p$ from the long-term average $uWUE_p$ for the 71 site-years and the four vegetation types; and (b) the mean, standard deviation (SD) of annual $uWUE_p$, and the coefficient of variation (CV) for the 17 sites.

The long-term average $uWUE_p$ was further compared with $uWUE_i$ calculated using equation 7 and values for λ_{cf}, C_a, and Γ. As reviewed in *Lloyd and Farquhar* [1994], λ_{cf} estimated from leaf gas exchange studies ranged from 400 to 900 mol/mol for croplands, from 250 to 1250 mol/mol for nontropical forests, and from 500 to 700 mol/mol for grasslands. The corresponding $uWUE_i$ derived from λ_{cf} ranged from 10.01 to 15.14 g C·hPa$^{0.5}$/kg H_2O for croplands, and the range of $uWUE_i$ values among forests was large, from 8.56 to 19.15 g C·hPa$^{0.5}$/kg H_2O, and for grasslands the range was much smaller, only from 11.44 to 13.54 g C·hPa$^{0.5}$/kg H_2O. Comparing the long-term average $uWUE_p$ with the upper and lower estimates of the $uWUE_i$ noted above, the distribution of the long-term

average $uWUE_p$ is broadly consistent with the range of $uWUE_i$ values for these C3 plants at the 16 of 17 sites examined (Figure 3). Excluding the US-Ha1 site due to the biomass removal, the long-term average $uWUE_p$ ranged from 11.5 to 15.1 g C·hPa$^{0.5}$/kg H_2O for the 15 remaining sites and the difference in the mean $uWUE_p$ among the four vegetation types was less than 1.0 g C·hPa$^{0.5}$/kg H_2O, which was much smaller than the difference among sites of the same vegetation type, of about 2.7–3.5 g C·hPa$^{0.5}$/kg H_2O. Similarly, the difference in the estimated mean $uWUE_i$ values among the three vegetation types was less than 1.4 g C·hPa$^{0.5}$/kg H_2O and the difference in the upper and lower estimates was larger, from 2.1 g C·hPa$^{0.5}$/kg H_2O for grasslands to 10.6 g C·hPa$^{0.5}$/kg H_2O for forests. Table 2 shows a comparison of the mean $uWUE_p$ and $uWUE_i$ values for the four vegetation types excluding the US-Ha1 site. The difference between $uWUE_p$ and $uWUE_i$ varied from 0.35 to 1.38 g C·hPa$^{0.5}$/kg H_2O. The relative difference is no more than 4% for three of the four vegetation types, and the largest relative difference between the two is 10.5% for evergreen needle leaf forests (Table 2). The broad consistency between $uWUE_p$ and $uWUE_i$ and their similar values for C3 plants lend considerable additional support for using the quantile regression technique to estimate the long-term average $uWUE_p$, and hence ET partitioning, for sites where flux data are readily available.

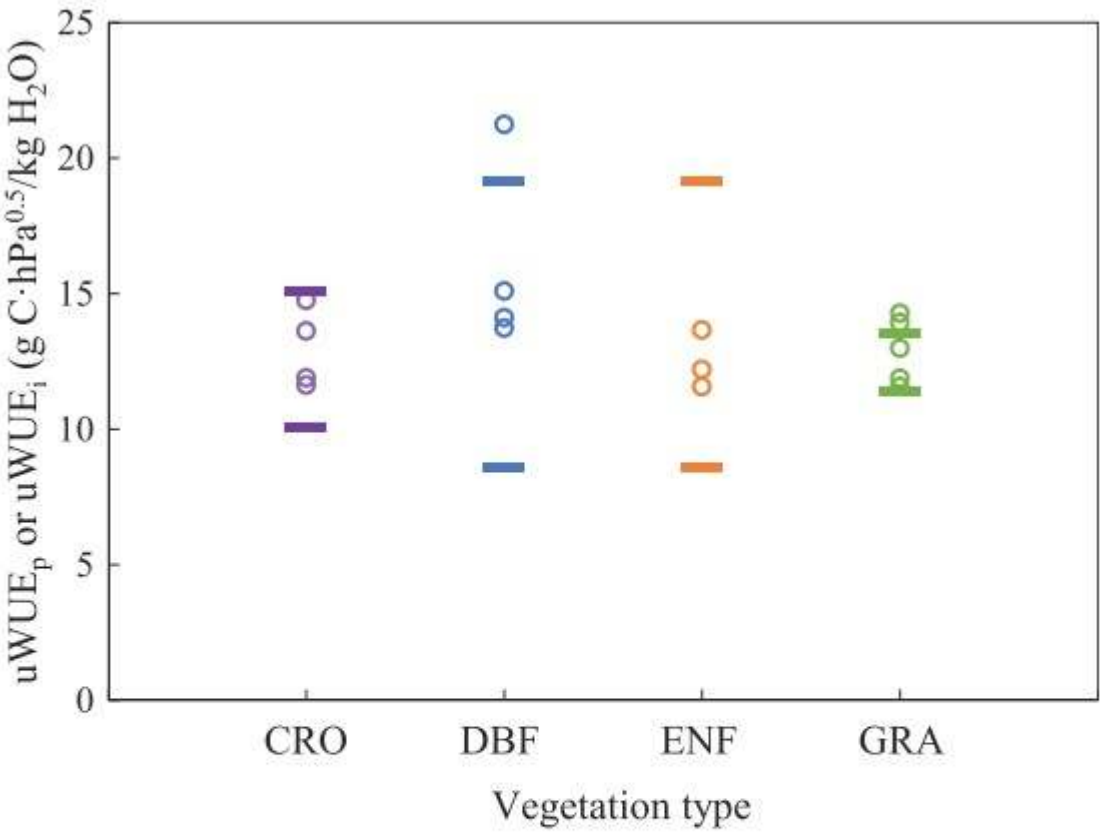

Figure 3. A comparison of the long-term average potential uWUE (circles) at the ecosystem scale ($uWUE_p$) for the 16 sites with C3 plants and the uWUE at the leaf scale ($uWUE_i$) for the four vegetation types (CRO = croplands, DBF = deciduous broadleaf forests, ENF = evergreen needle leaf forests, GRA = grasslands). The short horizontal bars represent the upper and lower estimates of $uWUE_i$ based on λ_{cf} values from *Lloyd and Farquhar* [1994].

Table 2. A Comparison of the Estimated Long-Term Average $uWUE_p$ (g C·hPa$^{0.5}$/kg H_2O) at the Ecosystem Scale and the Midrange $uWUE_i$ Values (g C·hPa$^{0.5}$/kg H_2O) at the Leaf Scale Based on λ_{cf} Values From *Lloyd and Farquhar* [1994] for the 15 Sites With C3 Plants Excluding the US-Ha1 Site[a]

Vegetation Type	$uWUE_p$	$uWUE_i$	Difference (%)
Croplands	12.97	12.62	2.7
Deciduous broadleaf forests	13.40	13.86	3.4
Evergreen needle leaf forests	12.48	13.86	10.5
Grasslands	12.93	12.49	3.5

[a]The difference (%) is the absolute difference between $uWUE_p$ and $uWUE_i$ expressed as percent of the average of the estimated $uWUE_p$ and $uWUE_i$ values.

3.2 Estimation of the Apparent uWUE and T/ET

The annual $uWUE_a$ and T/ET varied greatly among the 71 site-years with different vegetation types, as shown in Figure 4. T/ET was higher for croplands (corn and soybean) than other vegetation types on average. Because of the mixed C3/C4 vegetation at the US-Bo1 site, the annual $uWUE_a$ and T/ET had higher interannual variations. Except for the US-Bo1 site, the $uWUE_a$ ranged from 11.83 to 14.61 g C·hPa$^{0.5}$/kg H_2O and the T/ET ranged from 0.62 to 0.75 and was 0.69 on average for corn site-years, which were much higher than other vegetation types. For the soybean site-years, the $uWUE_a$ was much lower than corn site-years, ranging from 7.18 to 8.41 g C·hPa$^{0.5}$/kg H_2O and T/ET was from 0.53 to 0.69 and the average T/ET was 0.62. Though the $uWUE_a$ of deciduous broadleaf forests was relatively high, about 8.50 g C·hPa$^{0.5}$/kg H_2O, the corresponding T/ET was the smallest, only 0.52 on average, especially for US-Ha1, which ranged from only 0.34 to 0.52 during the recovery period from 2000 to 2006. Among evergreen needle leaf forests, US-NC2 showed higher $uWUE_a$ (8.68 g C·hPa$^{0.5}$/kg H_2O) and T/ET (0.64) than other two sites, and the average $uWUE_a$ and T/ET were 6.91 g C·hPa$^{0.5}$/kg H_2O and 0.56, respectively. The variation in $uWUE_a$ among grasslands was small, and T/ET varied from 0.46 to 0.71 with an average of 0.59 among all the site-years for grasslands. Apart from the difference in the long-term average $uWUE_p$ among all the sites, climatic and biotic factors, such as water and energy availability, contributed to the variation in the annual $uWUE_a$ and T/ET.

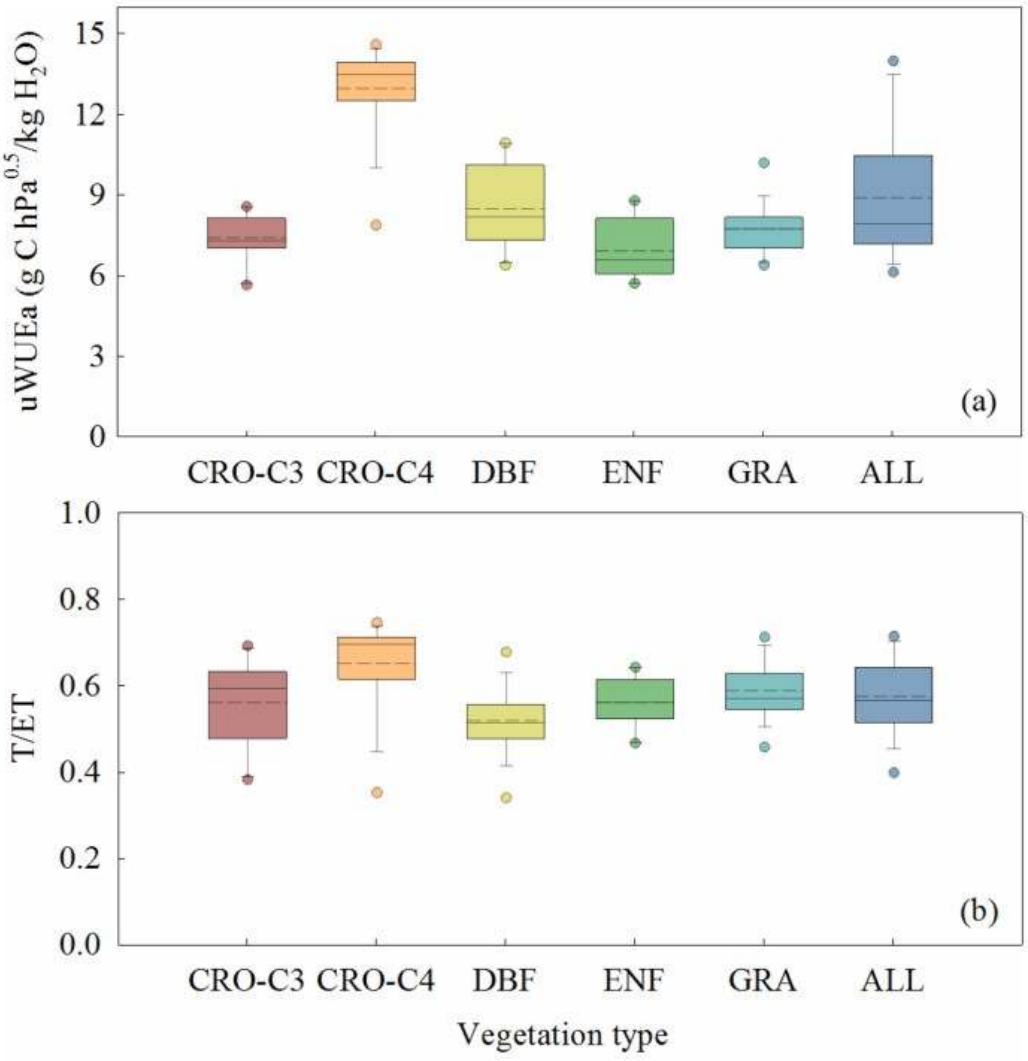

Figure 4. Frequency distribution of (a) the apparent uWUE ($uWUE_a$) and (b) T/ET for the 71 site-years. The C3 plant was soybean and C4 plant was corn. The dashed and solid lines in the boxes refer to the average and median values, respectively.

The estimated annual T/ET was further compared with the reported annual T/ET values from a compilation of previous ET partitioning studies in *Schlesinger and Jasechko* [2014]. Our estimated annual T/ET (0.52 ± 0.08) is lower than that reported (0.67 ± 0.14) for deciduous broadleaf forests. The range in T/ET (0.41–0.68) in this study, however, is within the range for this vegetation type (0.4–0.86) reported in *Schlesinger and Jasechko* [2014], except for the year 2000 at the US-Ha1 site (T/ET = 0.34), for reasons given in section 3.1. The difference in the annual T/ET between evergreen needle leaf forests and grasslands is small in this study (0.59 ± 0.06 and 0.56 ± 0.05) in comparison to that reported in *Schlesinger and Jasechko* [2014] (0.55 ± 0.15 and 0.57 ± 0.19). Thus, our estimated annual T/ET is fairly similar in value when compared to that reported in the literature for the three different vegetation types (DBF, ENF, and GRA). This broad comparison

in terms of T/ET lends support to this new method for ET partitioning, although additional validation of this method is required when synchronized measurements of T and ET are available for these and other flux sites.

Seasonal and interannual variations in T/ET were estimated at the daily scale. For example, the daily time series of T/ET at the US-Ne3 site are shown in Figure 5. The vegetation at this site was an annual rotation between corn (2001, 2003, and 2005) and soybean (2002 and 2004). The seasonal pattern of T/ET for corn and soybean is noticeably different. For soybean, there appears to be high-frequency fluctuations when T/ET is less than 0.4 and its growth rate is slower than that for corn; for corn, the fluctuations are much smaller at the beginning of the growing season. The rate of decrease in T/ET is quite similar for both soybean and corn toward the end of the growing season though. Daily variation in T/ET follows a single-peak pattern for US-Ne3 within a year, from about 0.05–0.2 in the early growing season to more than 0.8 during the mature period, and these results were similar to those reported by *Scanlon and Kustas* [2012], which estimated daily T/ET for a corn site using high-frequency flux data based on the correlation analysis method [*Scanlon and Kustas*, 2010]. The estimated T/ET showed variation from day to day and this high-frequency variation may be attributed to the effect of climatic or biotic factors, and data uncertainty can also lead to high variation in the estimated daily T/ET. Similarly, the estimated daily T and ET based on scaled sap flux and eddy covariance measurements also show high-frequency variations at the Duke Forest Hardwoods site [*Oishi et al*., 2008]. During the mature period of dense corn, daily T/ET was more than 0.8, which was consistent with the values reported by sap flow measurements for corn [*Bethenod et al*., 2000]. The daily T/ET among the 17 sites was greater than 0.9 and close to unity for several days during the growing season, and this resulted from the assumption that soil evaporation was negligible and transpiration was equal to evapotranspiration sometimes during the growing season.

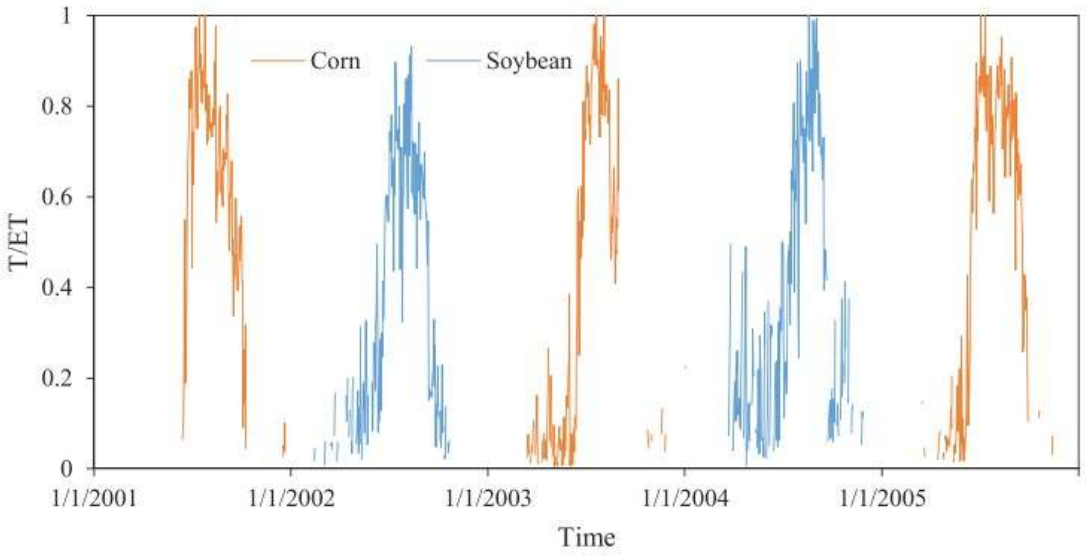

Figure 5. Seasonal and interannual variations in T/ET at the daily scale at the US-Ne3 site. The vegetation at this site was an annual rotation between corn and soybean. Parts of T/ET data were excluded following the data processing.

3.3 Effect of Vegetation on T/ET

Based on the uWUE method, the $uWUE_a$ and T/ET were estimated for each 8 day period and T/ET was related to the 8 day EVI for each site-year. Both EVI and T/ET range from 0 to 1 for most terrestrial ecosystems, and there is a linear relationship between EVI and T/ET. For example, R^2 between EVI and T/ET in 2005 at the US-Ne3 site was 0.85 (Figure 6). Thus, linear relationships between EVI and T/ET could be used to assess the controlling effect of vegetation coverage over ET partitioning for the 71 site-years. The linear regression showed that R^2 between 8 day EVI and T/ET was about 0.75 on average, and it was larger than 0.8 for more than 50% of the 71 site-years (Figure 7). EVI could explain about 83% of the variation in T/ET for croplands, and explain more than 90% for 9 of the 25 site-years. R^2 between EVI and T/ET for the deciduous broadleaf forests and grasslands was about 0.77, and only 0.37 for evergreen needle leaf forests (Figure 7). The linear relationship between EVI and T/ET was much weaker for evergreen needle leaf forests than for other vegetation types, indicating that the change in T/ET is more strongly related to vegetation coverage for deciduous plants, grass, and crops than evergreen plants. In addition, the lower R^2 value for the evergreen needle leaf forests may be related to the comparatively small seasonal amplitude in EVI. The magnitude of variation in EVI and T/ET was large, and the seasonal variations in EVI and T/ET were more consistent for croplands than other vegetation types, resulting in a strong relationship between vegetation coverage and ET partitioning. Irrigated site (US-Ne2) showed higher annual T/ET (0.70) and stronger vegetation controlling effect ($R^2 = 0.81$) than the rainfed site (US-Ne3) because of better water utilization. Annual T/ET was 0.67 and R^2 was 0.73 on average for the US-Ne3 site.

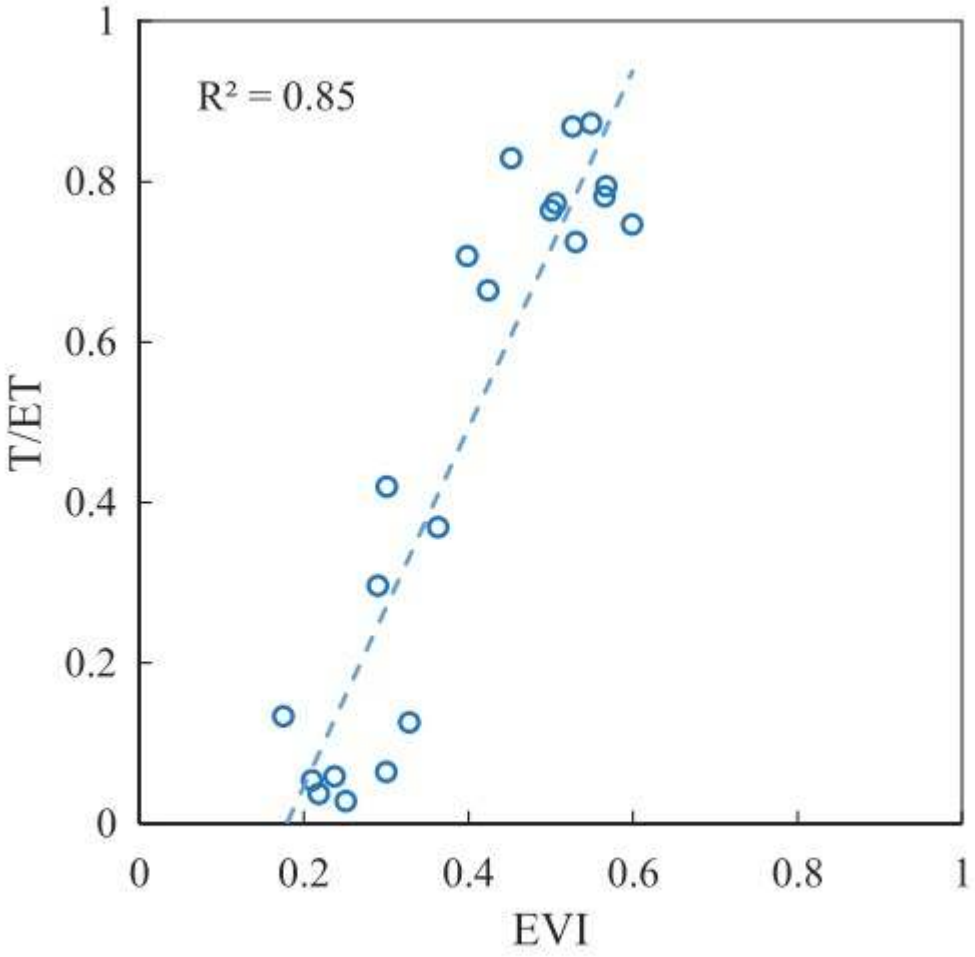

Figure 6. The relationship between EVI and T/ET at the 8 day scale in 2005 at the US-Ne3 site.

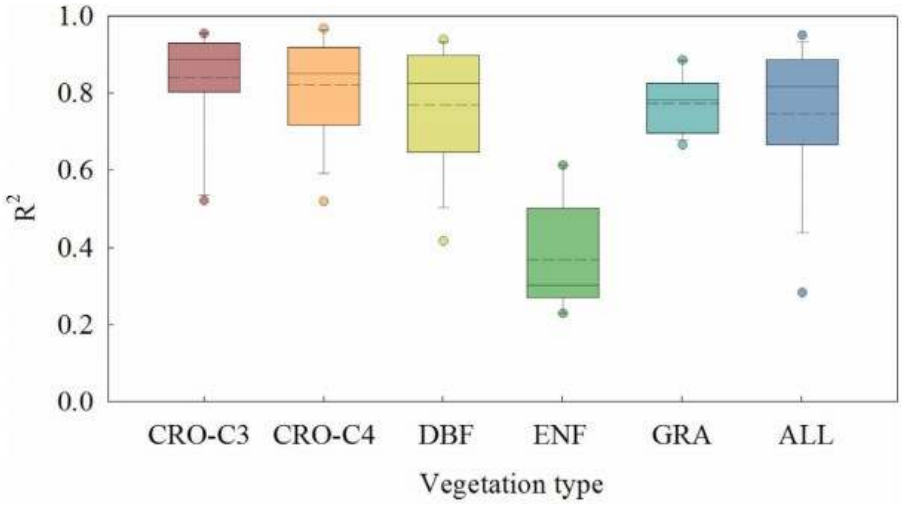

Figure 7. Frequency distribution of the coefficients of determination (R^2) between 8 day EVI and T/ET for the 71 site-years. The C3 plant was soybean and C4 plant was corn. The dashed and solid lines in the boxes refer to the average and median values, respectively.

The seasonal and interannual variations in 8 day EVI and T/ET are shown in Figure 8 for four sites, namely US-Ne3 (CRO), US-Ha1 (DBF), US-Arc (GRA), and CA-NS3 (ENF). US-Ne3 is a corn-soybean rotation site, and R^2 value ranged from 0.52 to 0.87 for the 5 site-years and was 0.74 overall for the site. The peak value of T/ET was about 0.89 and that of EVI was about 0.64 in the corn years, i.e., 2001, 2003, and 2005 (Figure 8a). However, T/ET and EVI changed greatly between soybean years, and the differences in peak values of T/ET and EVI were more than 0.10 between 2002 and 2004, because 2002 was a severe drought year and had great impact on this rainfed site [*Svoboda et al*., 2002]. Although the shape and range of EVI changed only slightly from 2000 to 2006 for the US-Ha1 site, the peak values of T/ET increased from about 0.4 in 2000 to more than 0.8 in 2005 and 2006 (Figure 8b). The low T/ET from 2000 to 2004 may be a result of the commercial harvest in the summer of 2000 when a large amount of aboveground woody biomass was removed [*Urbanski et al*., 2007]. However, the seasonal pattern and peak values of EVI hardly changed during the period from 2000 to 2006 because the EVI at the 500 m resolution (about 250 m around the tower) was not sensitive to the harvest which occurred 300 m to the S-SE of the tower. Estimated T/ET was sensitive to the removal of biomass and was subsequently increased with plant recovery from 2000 to 2006 since forest flux tower has large footprints of flux measurements, ranging from hundreds of meters to 1 km in radius [*Kljun et al*., 2002]. As for the site US-ARc in Figure 8c, the decrease in T/ET was related to the decline in EVI from 2005 to 2006, and the dual-peak pattern of T/ET was consistent with that of EVI, resulting from low occurrence of precipitation during the late summer in 2006 [*Wagle et al*., 2014]. For the three deciduous sites, T/ET showed a good linear relationship with EVI and vegetation played a dominant role in T/ET during the growing season. However, the linear relationship between EVI and T/ET was weak at the CA-NS3 site because the vegetation cover changed slightly within a year

(Figure 8d), while T/ET was largely driven by other climatic and biotic factors, such as temperature, solar radiation, and soil water content [*Zhu et al*., 2015].

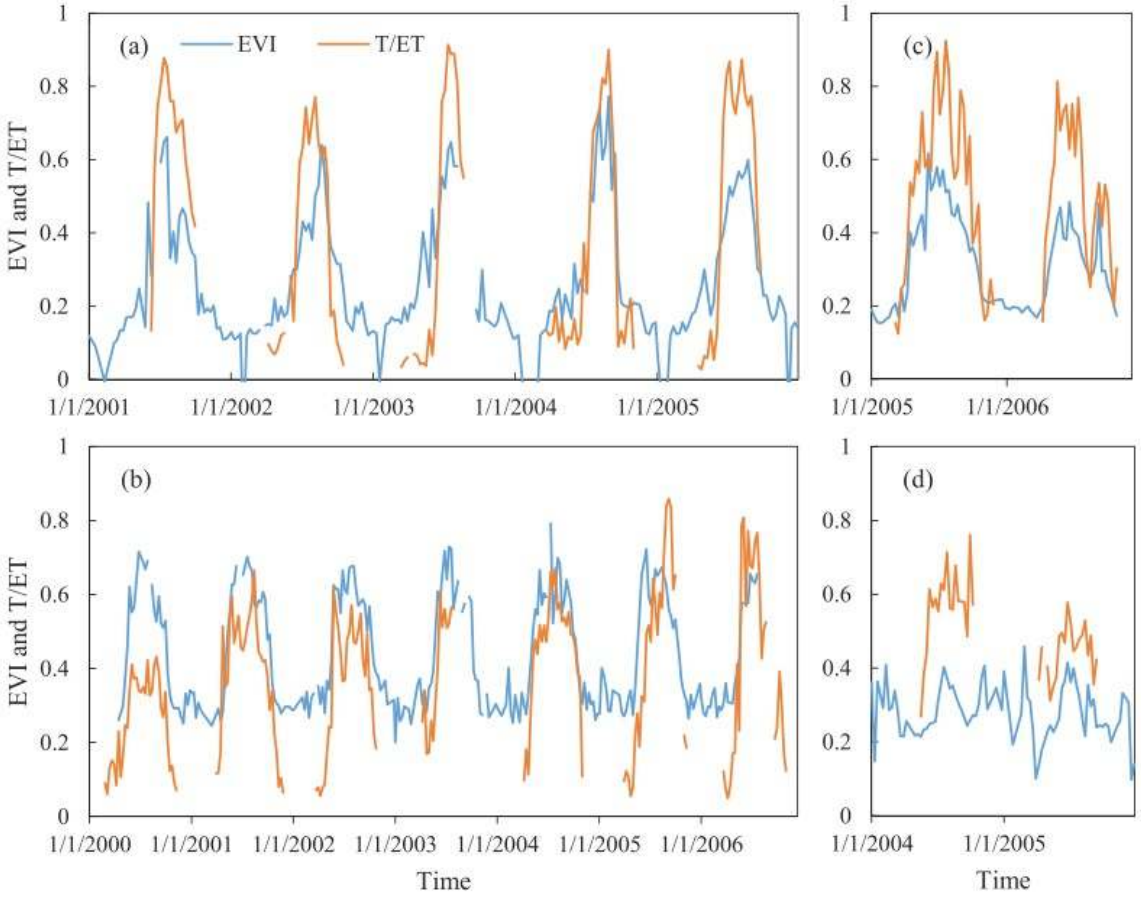

Figure 8. Seasonal and interannual variations in EVI and T/ET at the 8 day scale for the site (a) US-Ne3 (CRO), (b) US-Ha1 (DBF), (c) US-ARc (GRA), and (d) CA-NS3 (ENF). Some EVI observations were not available due to the data quality issues and parts of T/ET data were excluded following the data processing.

3.4 Implications and Limitations of This Study

This study shows that the T/ET ratio at different scales can be estimated based on the $uWUE_p$ and $uWUE_a$ inferred from half-hourly flux data. This method can be easily used at other flux sites to estimate the $uWUE_p$ and $uWUE_a$ for these sites. Thus, temporal and spatial variations in T/ET based on the FluxNet observations can be continuously estimated to monitor ecosystem dynamics and hydrological responses to climatic change. In addition, the spatially distributed T/ET products could be further enhanced from the $uWUE_p$ and $uWUE_a$ data sets at the global scale. Moreover, the linear relationship between EVI and T/ET for deciduous vegetation showed that the majority of the variation in T/ET could be explained by EVI and this relationship could be used to develop an empirical ET partitioning model and to interpret the variation in T/ET for deciduous vegetation.

However, there are some limitations in this study. First, the ET partitioning method has not been validated with direct observations of E and T because of the lack of in situ measurements in these sites. Second, the uncertainty in GPP measurements was not considered in this study. Since GPP was not observed directly and was estimated from net ecosystem exchange and respiration, the uncertainty in GPP (less than 10%) would result in some uncertainty in the $uWUE_a$ and hence T/ET. Third, possible violation of the two assumptions that underpin the proposed method could lead to uncertainty in the estimated T/ET, although we have provided some empirical support for these two assumptions in this paper. The first one was that the $uWUE_p$ is constant for each site, and this assumption may be violated when the site has several vegetation types, as explained in section 3.1. The $uWUE_p$ may also change when atmospheric CO_2 concentrations vary greatly because equation 7 showed that the $uWUE_p$ was proportional to the square root of CO_2 concentrations. More specifically, if we assume the mean CO_2 concentrations is 380 ppm and the CO_2 compensation point is 50 ppm, and the seasonal variation in the CO_2 concentrations is about 13.8 ± 0.7 ppm, as reported in *Graven et al*. [2013], the uncertainty in the $uWUE_p$ would be less than 3%. Thus, the seasonal variation in atmospheric CO_2 could lead to some variation in the $uWUE_p$ and the CO_2 fertilization effect should be taken into account when CO_2 concentrations changed considerably over a long period. The second assumption that T would be equal to ET sometimes during the growing season may be violated where vegetation is sparse and soil evaporation cannot be ignored even during the peak growing season, and the $uWUE_p$ may be underestimated and T/ET is overestimated. Thus, the estimated $uWUE_p$ should be revised for these ecosystems by adjusting the estimated T/ET using other methods, such as the isotope technique or in situ measurement techniques.

4 Conclusions

This study used half-hourly flux tower measurements from 17 AmeriFlux sites to develop a new ET partitioning method based on the concept of the underlying water use efficiency. The ratio of $uWUE_a$ over $uWUE_p$ was proposed for estimating T/ET for four vegetation types. This method was sound in principle and easy to apply in practice, and could be widely implemented using data from global flux tower networks.

The $uWUE_p$ was stable for sites with a single vegetation type, and was broadly consistent with the uWUE at the leaf scale for the four C3 vegetation types, indicating that the 95th quantile regression technique was effective in estimating the $uWUE_p$. The difference in the mean $uWUE_p$ among different vegetation types was smaller than the variation in the $uWUE_p$ within a given vegetation type. C4 plants have much larger $uWUE_p$ and $uWUE_a$ than C3 plants because of their higher photosynthetic capacity and water use efficiency. The annual $uWUE_a$ and T/ET varied among different vegetation types, and croplands (except for the C3/C4 mixed site US-Bo1) showed higher T/ET than other vegetation types. The T/ET ratio was 0.69 for corn and 0.62 for soybean, followed by grasslands (0.60) and evergreen needle leaf forests (0.56), and

T/ET of deciduous broadleaf forests was only 0.52, which was the lowest of the four vegetation types considered. Time series of 8 day T/ET and EVI showed similar and consistent seasonal and interannual variations and there is a strong linear relationship between EVI and T/ET ($R^2 = 0.75$). EVI could explain 84% and 82% of the variations in T/ET for corn and soybean, respectively, and 77% for deciduous broadleaf forests and grasslands, and only 37% for evergreen needle leaf forests, indicating a strong controlling effect of vegetation coverage over ET partitioning for deciduous vegetation.

As the ET partitioning method provided a simple way to estimate T/ET, it could be further used for producing continuous T/ET data sets and monitoring ecosystem dynamics at the regional and global scales. Since EVI was closely related to T/ET ratio in deciduous ecosystems, the linear relationship between EVI and T/ET could be used to interpret the variation in T/ET.

Acknowledgments

We thank Kelly K. Caylor from the Princeton University for his valuable comments on an earlier version of the manuscript. The tower flux and meteorological data and the 8 day EVI data of the 17 flux sites used for the paper were available at the AmeriFlux network (http://public.ornl.gov/ameriflux) and the Earth Observation and Modeling Facility, University of Oklahoma (http://eomf.ou.edu/visualization/gmap/), respectively. We acknowledge the following AmeriFlux sites for their data records: US-Bo1, US-IB1, US-Ne1, US-Ne2, US-Ne3, US-Ha1, US-Moz, US-UMB, US-WCr, US-Arb, US-Arc, US-Goo, US-Var, US-Wlr, CA-NS3, CA-NS5, and US-NC2. In addition, funding for AmeriFlux data resources was provided by the U.S. Department of Energy's Office of Science. This paper is financially supported by the National Natural Science Foundation of China (91125018), National Key Science and Technology Project Fund from the Ministry of Science and Technology (MOST) during the 12th 5 year Project (2013BAB05B03), and the Research and Development Special Fund for Public Welfare Industry of the Ministry of Water Research in China (201301081).

References

Ashktorab, H., W. O. Pruitt, and K. T. Paw U (1994), Partitioning of evapotranspiration using lysimeter and micro-bowen-ratio system, *J. Irrig. Drain. Eng.*, 120(2), 450– 464, doi:10.1061/(ASCE)0733-9437(1994)120:2(450).

Baldocchi, D. (2014), Measuring fluxes of trace gases and energy between ecosystems and the atmosphere: The state and future of the eddy covariance method, *Global Change Biol.*, 20(12), 3600– 3609, doi:10.1111/gcb.12649.

Baldocchi, D. D., and Y. Ryu (2011), A synthesis of forest evaporation fluxes —from days to years—as measured with eddy covariance, in *Forest*

Hydrology and Biogeochemistry, vol. 216, pp. 101– 116, Springer, Netherlands.

Beer, C., M. Reichstein, P. Ciais, G. D. Farquhar, and D. Papale (2007), Mean annual GPP of Europe derived from its water balance, *Geophys. Res. Lett.*, 34, L05401, doi:10.1029/2006GL029006.

Beer, C., et al. (2009), Temporal and among-site variability of inherent water use efficiency at the ecosystem level, *Global Biogeochem. Cycles*, 23, GB2018, doi:10.1029/2008GB003233.

Bethenod, O., N. Katerji, R. Goujet, J. M. Bertolini, and G. Rana (2000), Determination and validation of corn crop transpirationby sap flow measurement under field conditions, *Theor. Appl. Climatol.*, 67(3–4), 153–160, doi:10.1007/s007040070004.

Bremnes, J. B. (2004), Probabilistic wind power forecasts using local quantile regression, *Wind Energy*, 7(1), 47– 54, doi:10.1002/we.107.

Cade, B. S., and B. R. Noon (2003), A gentle introduction to quantile regression for ecologists, *Front. Ecol. Environ.*, 1(8), 412– 420.

Cammalleri, C., G. Rallo, C. Agnese, G. Ciraolo, M. Minacapilli, and G. Provenzano (2013), Combined use of eddy covariance and sap flow techniques for partition of ET fluxes and water stress assessment in an irrigated olive orchard, *Agric. Water Manage.*, 120, 89– 97.

Choudhury, B. J., N. U. Ahmed, S. B. Idso, R. J. Reginato, and C. S. T. Daughtry (1994), Relations between evaporation coefficients and vegetation indexes studied by model simulations, *Remote Sens. Environ.*, 50(1), 1– 17.

Coulter, R. L., M. S. Pekour, D. R. Cook, G. E. Klazura, T. J. Martin, and J. D. Lucas (2006), Surface energy and carbon dioxide fluxes above different vegetation types within ABLE, *Agric. For. Meteorol.*, 136, 147– 158.

Cowan, I. R., and G. D. Farquhar (1977), Stomatal function in relation to leaf metabolism and environment, *Symp. Soc. Exp. Biol.*, 31, 471– 505.

Desai, A. R., P. V. Bolstad, B. D. Cook, K. J. Davis, and E. V. Carey (2005), Comparing net ecosystem exchange of carbon dioxide between an old-growth and mature forest in the upper Midwest, USA, *Agric. For. Meteorol.*, 128(1-2), 33– 55.

Donatelli, M., G. Bellocchi, and L. Carlini (2006), Sharing knowledge via software components: Models on reference evapotranspiration, *Eur. J. Agron.*, 24(2), 186– 192.

Ehleringer, J., and O. Bjorkman (1977), Quantum yields for CO_2 uptake in C3 and C4 plants, *Plant Physiol.*, 59(1), 86– 90, doi:10.1104/pp.59.1.86.

Ferreira, L. G., H. Yoshioka, A. Huete, and E. E. Sano (2003), Seasonal landscape and spectral vegetation index dynamics in the Brazilian Cerrado: An analysis within the Large-Scale Biosphere-Atmosphere Experiment in

Amazonia (LBA), *Remote Sens. Environ.*, 87(4), 534– 550, doi:10.1016/j.rse.2002.09.003.

Furbank, R., and W. Taylor (1995), Regulation of photosynthesis in C3 and C4 plants: A molecular approach, *Plant Cell*, 7(7), 797– 807, doi:10.1105/tpc.7.7.797.

Gao, X., A. R. Huete, W. G. Ni, and T. Miura (2000), Optical-biophysical relationships of vegetation spectra without background contamination, *Remote Sens. Environ.*, 74, 609– 620.

Glenn, E. P., P. L. Nagler, and A. R. Huete (2010), Vegetation Index Methods for Estimating Evapotranspiration by Remote Sensing, *Surv. Geophys.*, 31(6), 531– 555.

Glenn, E. P., C. M. U. Neale, D. J. Hunsaker, and P. L. Nagler (2011), Vegetation index-based crop coefficients to estimate evapotranspiration by remote sensing in agricultural and natural ecosystems, *Hydrol. Processes*, 25(26), 4050– 4062.

Good, S. P., K. Soderberg, K. Guan, E. G. King, T. M. Scanlon, and K. K. Caylor (2014), δ2H isotopic flux partitioning of evapotranspiration over a grass field following a water pulse and subsequent dry down, *Water Resour. Res.*, 50, 1410– 1432, doi:10.1002/2013WR014333.

Gough, C. M., C. S. Vogel, H. P. Schmid, H. B. Su, and P. S. Curtis (2008), Multi-year convergence of biometric and meteorological estimates of forest carbon storage, *Agric. For. Meteorol.*, 148, 158– 170.

Goulden, M. L., G. C. Winston, A. M. S. McMillan, M. E. Litvak, E. L. Read, A. V. Rocha, and J. R. Elliot (2006), An eddy covariance mesonet to measure the effect of forest age on land-atmosphere exchange, *Global Change Biol.*, 12(11), 2146– 2162, doi:10.1111/j.1365-2486.2006.01251.x.

Graven, H. D. et al. (2013), Enhanced seasonal exchange of CO_2 by northern ecosystems since 1960, *Science*, 341(6150), 1085– 1089, doi:10.1126/science.1239207.

Griffis, T. J. (2013), Tracing the flow of carbon dioxide and water vapor between the biosphere and atmosphere: A review of optical isotope techniques and their application, *Agric. For. Meteorol.*, 174–175, 85– 109, doi:10.1016/j.agrformet.2013.02.009.

Gu, L., et al. (2007), Influences of biomass heat and biochemical energy storages on the land surface fluxes and diurnal temperature range, *J. Geophys. Res.*, 112, D02107, doi:10.1029/2006JD007425.

Hollinger, S. E., C. J. Bernacchi, and T. P. Meyers (2005), Carbon budget of mature no-till ecosystem in North Central Region of the United States, *Agric. For. Meteorol.*, 130, 59– 69.

Huang, M., B. Vieux, S. Caliskan, T. Grout, W. Liu, Y. Hong, and S. I. Khan (2010), Actual evapotranspiration estimation for different land use and land

cover in urban regions using Landsat 5 data, *J. Appl. Remote Sens.*, 4(1), 041873.

Huete, a., K. Didan, T. Miura, E. P. Rodriguez, X. Gao, and L. G. Ferreira (2002), Overview of the radiometric and biophysical performance of the MODIS vegetation indices, *Remote Sens. Environ.*, 83(1–2), 195– 213, doi:10.1016/S0034-4257(02)00096-2.

Jasechko, S., Z. D. Sharp, J. J. Gibson, S. J. Birks, Y. Yi, and P. J. Fawcett (2013), Terrestrial water fluxes dominated by transpiration., *Nature*, 496(7445), 347– 350, doi:10.1038/nature11983.

Jin, C., X. Xiao, L. Merbold, A. Arneth, E. Veenendaal, and W. L. Kutsch (2013), Phenology and gross primary production of two dominant savanna woodland ecosystems in Southern Africa, *Remote Sens. Environ.*, 135, 189–201, doi:10.1016/j.rse.2013.03.033.

Kljun, N., M. W. Rotach, and H. P. Schmid (2002), A three-dimensional backward lagrangian footprint model for a wide range of boundary-layer stratifications, *Boundary Layer Meteorol.*, 103(2), 205– 226.

Kool, D., N. Agam, N. Lazarovitch, J. L. Heitman, T. J. Sauer, and A. Ben-Gal (2014), A review of approaches for evapotranspiration partitioning, *Agric. For. Meteorol.*, 184, 56– 70, doi:10.1016/j.agrformet.2013.09.003.

Lawrence, D. M., P. E. Thornton, K. W. Oleson, and G. B. Bonan (2007), The partitioning of evapotranspiration into transpiration, soil evaporation, and canopy evaporation in a GCM: Impacts on land-atmosphere interaction, *J. Hydrometeorol.*, 8(4), 862– 880, doi:10.1175/JHM596.1.

Lloyd, J. (1991), Modeling stomatal responses to environment in macadamia: Integrifolia, *Aust. J. Plant Physiol.*, 18(6), 649– 660, doi:10.1071/PP9910649.

Lloyd, J., and G. D. Farquhar (1994), International association for ecology 13C discrimination during CO_2 assimilation by the terrestrial biosphere, *Oecologia*, 99(3), 201– 215.

Matamala, R., J. D. Jastrow, R. M. Miller, and C. T. Garten (2008), Temporal changes in C and N stocks of restored prairie: Implications for C sequestration strategies, *Ecol. Appl.*, 18(6), 1470– 1488.

Meyers, T. P., and S. E. Hollinger (2004), An assessment of storage terms in the surface energy balance of maize and soybean, *Agric. For. Meteorol.*, 125(1-2), 105– 115, doi:10.1016/j.agrformet.2004.03.001.

Murray, R. S., P. L. Nagler, K. Morino, and E. P. Glenn (2009), an empirical algorithm for estimating agricultural and riparian evapotranspiration using MODIS enhanced vegetation index and ground measurements of ET. II. Application to the Lower Colorado River, U.S., *Remote Sens.*, 1(4), 1125–1138.

Nagler, P. L., J. Cleverly, E. Glenn, D. Lampkin, A. Huete, and Z. Wan (2005a), Predicting riparian evapotranspiration from MODIS vegetation indices and

meteorological data, *Remote Sens. Environ.*, 94, 17– 30, doi:10.1016/j.rse.2004.08.009.

Nagler, P., Scott, R., Westenburg, C., Cleverly, J., Glenn, E., & Huete, A. (2005b). Evapotranspiration on western U.S. rivers estimated using the enhanced vegetation index from MODIS and data from eddy covariance and Bowen ratio flux towers, *Remote Sens. Environ.*, 97, 337– 351.

Nagler, P. L., K. Morino, R. S. Murray, J. Osterberg, and E. P. Glenn (2009), An Empirical algorithm for estimating agricultural and riparian vapotranspiration using MODIS enhanced vegetation index and ground measurements of ET. I. Description of method, *Remote Sens.*, 1(4), 1273– 1297.

Noormets, A., M. J. Gavazzi, S. G. McNulty, J. C. Domec, G. E. Sun, J. S. King, and J. Chen (2010), Response of carbon fluxes to drought in a coastal plain loblolly pine forest, *Global Change Biol.*, 16(1), 272– 287.

Oishi, A. C., R. Oren, and P. C. Stoy (2008), Estimating components of forest evapotranspiration: A footprint approach for scaling sap flux measurements, *Agric. For. Meteorol.*, 148(11), 1719– 1732.

Reichstein, M., et al. (2005), On the separation of net ecosystem exchange into assimilation and ecosystem respiration: Review and improved algorithm, *Global Change Biol.*, 11(9), 1424– 1439, doi:10.1111/j.1365-2486.2005.001002.x.

Running, S. W., and J. C. Coughlan (1988), A general model of forest ecosystem processes for regional applications I. Hydrologic balance, canopy gas exchange and primary production processes, *Ecol. Modell.*, 42(2), 125– 154.

Scanlon, T. M., and W. P. Kustas (2010), Partitioning carbon dioxide and water vapor fluxes using correlation analysis, *Agric. For. Meteorol.*, 150(1), 89– 99, doi:10.1016/j.agrformet.2009.09.005.

Scanlon, T. M., and W. P. Kustas (2012), Partitioning evapotranspiration using an eddy covariance-based technique: Improved assessment of soil moisture and land–atmosphere exchange dynamics, *Vadose Zone J.*, 11(3), doi:10.2136/vzj2012.0025.

Scanlon, T. M., and P. Sahu (2008), On the correlation structure of water vapor and carbon dioxide in the atmospheric surface layer: A basis for flux partitioning, *Water Resour. Res.*, 44, W10418, doi:10.1029/2008WR006932.

Schlesinger, W. H., and S. Jasechko (2014), Transpiration in the global water cycle, *Agric. For. Meteorol.*, 189–190, 115– 117, doi:10.1016/j.agrformet.2014.01.011.

Suyker, A. E., S. B. Verma, G. G. Burba, and T. J. Arkebauer (2005), Gross primary production and ecosystem respiration of irrigated maize and irrigated soybean during a growing season, *Agric. For. Meteorol.*, 131(3), 180– 190.

Svoboda, M., et al. (2002), The drought monitor, *Bull. Am. Meteorol. Soc.*, 83(8), 1181– 1190.

Tans, P. (2015), *Trends in atmospheric carbon dioxide: National Oceanic and Atmospheric Administration, Earth System Research Laboratory (NOAA/ESRL)*. [Available at: www.esrl.noaa.gov/gmd/ccgg/trends/.]

Urbanski, S., C. Barford, S. Wofsy, C. Kucharik, E. Pyle, J. Budney, K. McKain, D. Fitzjarrald, M. Czikowsky, and J. W. Munger (2007), Factors controlling CO_2 exchange on timescales from hourly to decadal at Harvard Forest, *J. Geophys. Res.*, 112, G02020, doi:10.1029/2006JG000293.

Villegas, J. C., J. E. Espeleta, C. T. Morrison, D. D. Breshears, and T. E. Huxman (2014), Factoring in canopy cover heterogeneity on evapotranspiration partitioning: Beyond big-leaf surface homogeneity assumptions, *J. Soil Water Conserv.*, 69(3), 78A– 83A, doi:10.2489/jswc.69.3.78A.

Vogan, P. J., and R. F. Sage (2012), Effects of low atmospheric CO2 and elevated temperature during growth on the gas exchange responses of C3, C3-C4 intermediate, and C4 species from three evolutionary lineages of C4 photosynthesis, *Oecologia*, 169(2), 341– 352, doi:10.1007/s00442-011-2201-z.

Wagle, P., X. Xiao, M. S. Torn, D. R. Cook, R. Matamala, M. L. Fischer, C. Jin, J. Dong, and C. Biradar (2014), Sensitivity of vegetation indices and gross primary production of tallgrass prairie to severe drought, *Remote Sens. Environ.*, 152, 1– 14, doi:10.1016/j.rse.2014.05.010.

Wang, K., P. Wang, Z. Li, M. Cribb, and M. Sparrow (2007), A simple method to estimate actual evapotranspiration from a combination of net radiation, vegetation index, and temperature, *J. Geophys. Res.*, 112, D15107, doi:10.1029/2006JD008351.

Wang, L., K. K. Caylor, J. C. Villegas, G. A. Barron-Gafford, D. D. Breshears, and T. E. Huxman (2010), Partitioning evapotranspiration across gradients of woody plant cover: Assessment of a stable isotope technique, *Geophys. Res. Lett.*, 37, L09401, doi:10.1029/2010GL043228.

Wang, L., S. Niu, S. P. Good, K. Soderberg, M. F. McCabe, R. A. Sherry, Y. Luo, X. Zhou, J. Xia, and K. K. Caylor (2013), The effect of warming on grassland evapotranspiration partitioning using laser-based isotope monitoring techniques, *Geochim. Cosmochim. Acta*, 111, 28– 38, doi:10.1016/j.gca.2012.12.047.

Wang, L., S. P. Good, and K. K. Caylor (2014), Global synthesis of vegetation control on evapotranspiration partitioning, *Geophys. Res. Lett.*, 41, 6753–6757, doi:10.1002/2014GL061439.

Wang, P., and T. Yamanaka (2014), Application of a two-source model for partitioning evapotranspiration and assessing its controls in temperate

grasslands in central Japan, *Ecohydrology*, 7(2), 345– 353, doi:10.1002/eco.1352.

Wilson, K. B., P. J. Hanson, P. J. Mulholland, D. D. Baldocchi, and S. D. Wullschleger (2001), A comparison of methods for determining forest evapotranspiration and its components: Sap-flow, soil water budget, eddy covariance and catchment water balance, *Agric. For. Meteorol.*, 106(2), 153–168.

Wilson, T. B., and T. P. Meyers (2007), Determining vegetation indices from solar and photosynthetically active radiation fluxes, *Agric. For. Meteorol.*, 144(3), 160– 179.

Xu, L., and D. D. Baldocchi (2004), Seasonal variation in carbon dioxide exchange over a Mediterranean annual grassland in California, *Agric. For. Meteorol.*, 123(1), 79– 96.

Yi, C., K. J. Davis, P. S. Bakwin, A. S. Denning, N. Zhang, A. Desai, J. C. Lin, and C. Gerbig (2004), Observed covariance between ecosystem carbon exchange and atmospheric boundary layer dynamics at a site in northern Wisconsin, *J. Geophys. Res.*, 109, D08302, doi:10.1029/2003JD004164.

Young, M. H., T. G. Caldwell, D. G. Meadows, and L. F. Fenstermaker (2009), Variability of soil physical and hydraulic properties at the Mojave Global Change Facility, Nevada: Implications for water budget and evapotranspiration, *J. Arid Environ.*, 73(8), 733– 744, doi:10.1016/j.jaridenv.2009.01.015.

Yu, K., and R. A. Moyeed (2001), Bayesian quantile regression, *Stat. Probab. Lett.*, 54, 437– 447.

Zhang, X., M. A. Friedl, C. B. Schaaf, A. H. Strahler, J. C. F. Hodges, F. Gao, B. C. Reed, and A. Huete (2003), Monitoring vegetation phenology using MODIS, *Remote Sens. Environ.*, 84(3), 471– 475, doi:10.1016/S0034-4257(02)00135-9.

Zhou, L. et al. (2014a), Widespread decline of Congo rainforest greenness in the past decade., *Nature*, 509(7498), 86– 90, doi:10.1038/nature13265.

Zhou, S., B. Yu, Y. Huang, and G. Wang (2014b), The effect of vapor pressure deficit on water use efficiency at the subdaily time scale, *Geophys. Res. Lett.*, 41, 5005– 5013, doi:10.1002/2014GL060741.

Zhou, S., B. Yu, Y. Huang, and G. Wang (2015), Daily underlying water use efficiency for AmeriFlux sites, *J. Geophys. Res. Biogeosci.*, 120, 887– 902.

Zhu, X. J., G. R. Yu, Z. M. Hu, Q. F. Wang, H. L. He, J. H. Yan, H. M. Wang, and J. H. Zhang (2015), Spatiotemporal variations of T/ET (the ratio of transpiration to evapotranspiration) in three forests of Eastern China, *Ecol. Indic.*, 52, 411– 421, doi:10.1016/j.ecolind.2014.12.030.